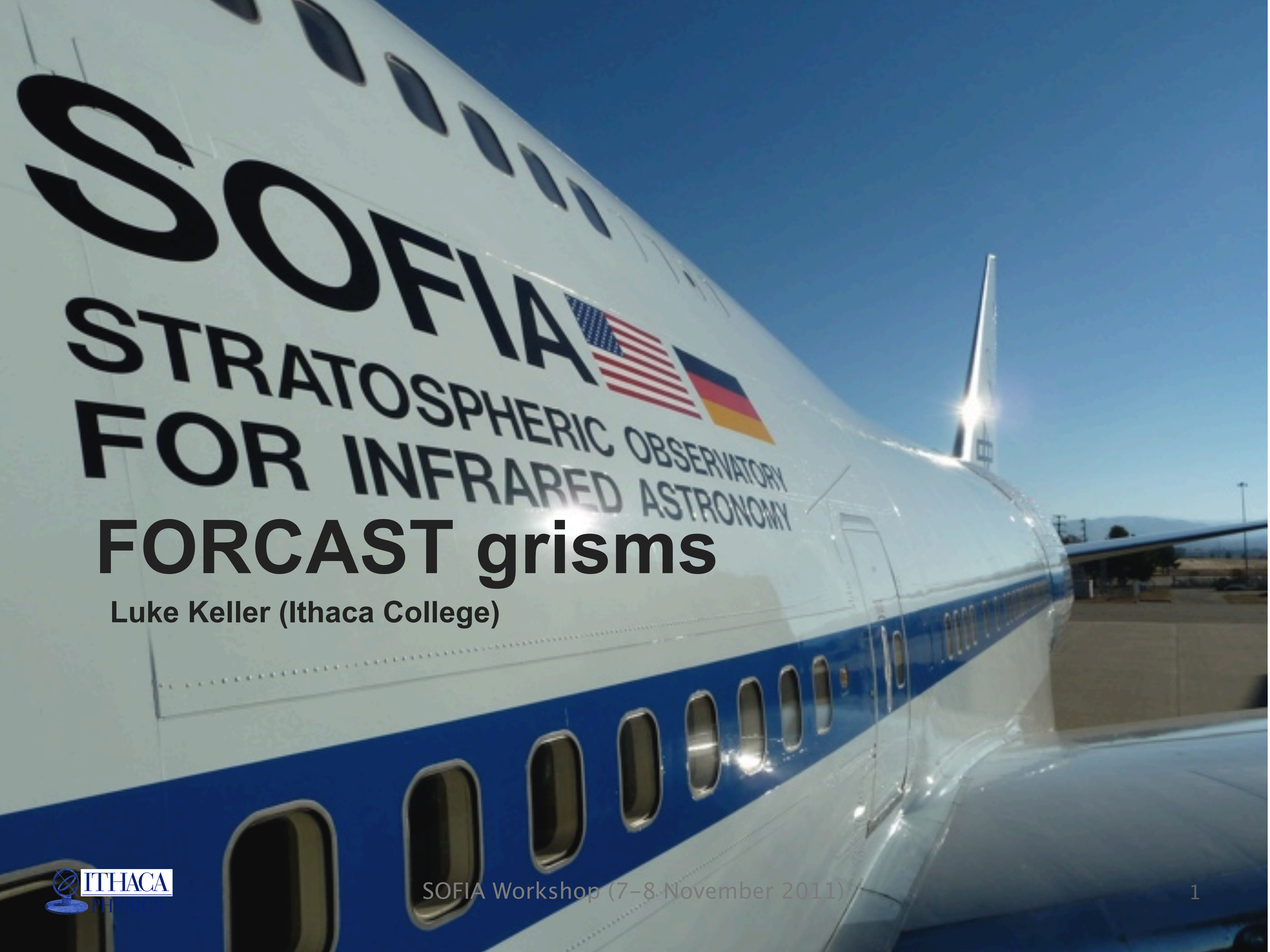

FORCAST grisms

Luke Keller (Ithaca College)

ITHACA PHYSICS

FORCAST grisms team

Luke Keller (PI, Ithaca College)

Kim Ennico (Co-I, NASA Ames & SWRI)

Dan Jaffe (Co-I, Univeristy of Texas at Austin)

Casey Deen (Co-I, University of Texas at Austin)

Tom Greene (Co-I, NASA Ames)

Greg Sloan (Co-I, Cornell University)

Terry Herter (Co-I, FORCAST PI, Cornell University)

Joe Adams (Co-I, FORCAST Project Scientist, Cornell University)

Today's plan:

- FORCAST grism spectroscopy design overview and brief history
- SOFIA Cycle 1 FORCAST grism observing modes
- Sample data (from lab tests)
- Data artifacts ("jailbar" pattern, interference fringing)
- Observation set-up: source acquisition, field rotation
- Pointed observations & mapping in extended sources
- Data products and data reduction steps
- Calibration: wavelength & flux calibration, telluric

Please keep in mind:

FORCAST's grism spectroscopy modes have undergone extensive testing in the lab, but have not been tested in flight (hance shared-risk offering in Cycle-1). Many of the details described here are plans and best estimates to be worked out in finer detail during test flights.

FORCAST grism design overview: layout

Grisms in existing imaging filter wheels

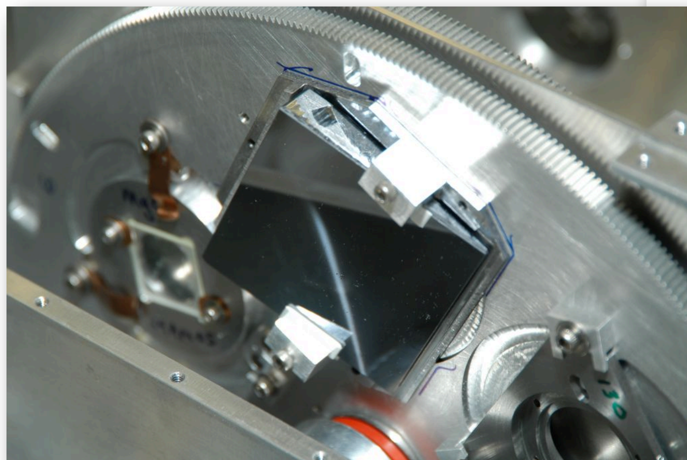

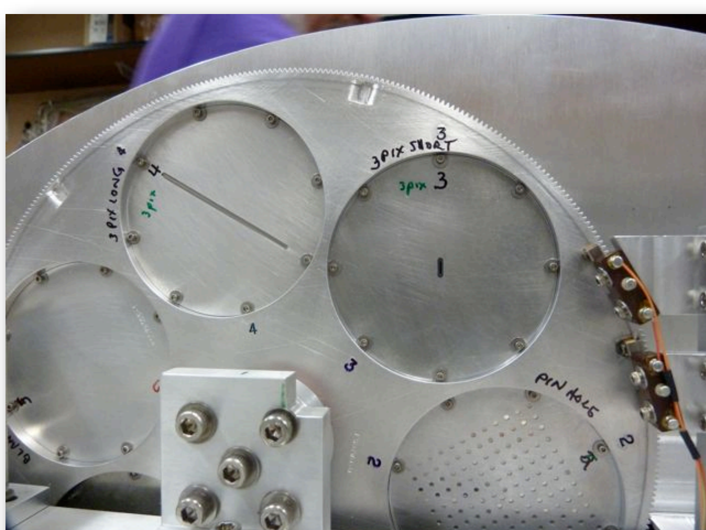

Slits in existing aperture wheel

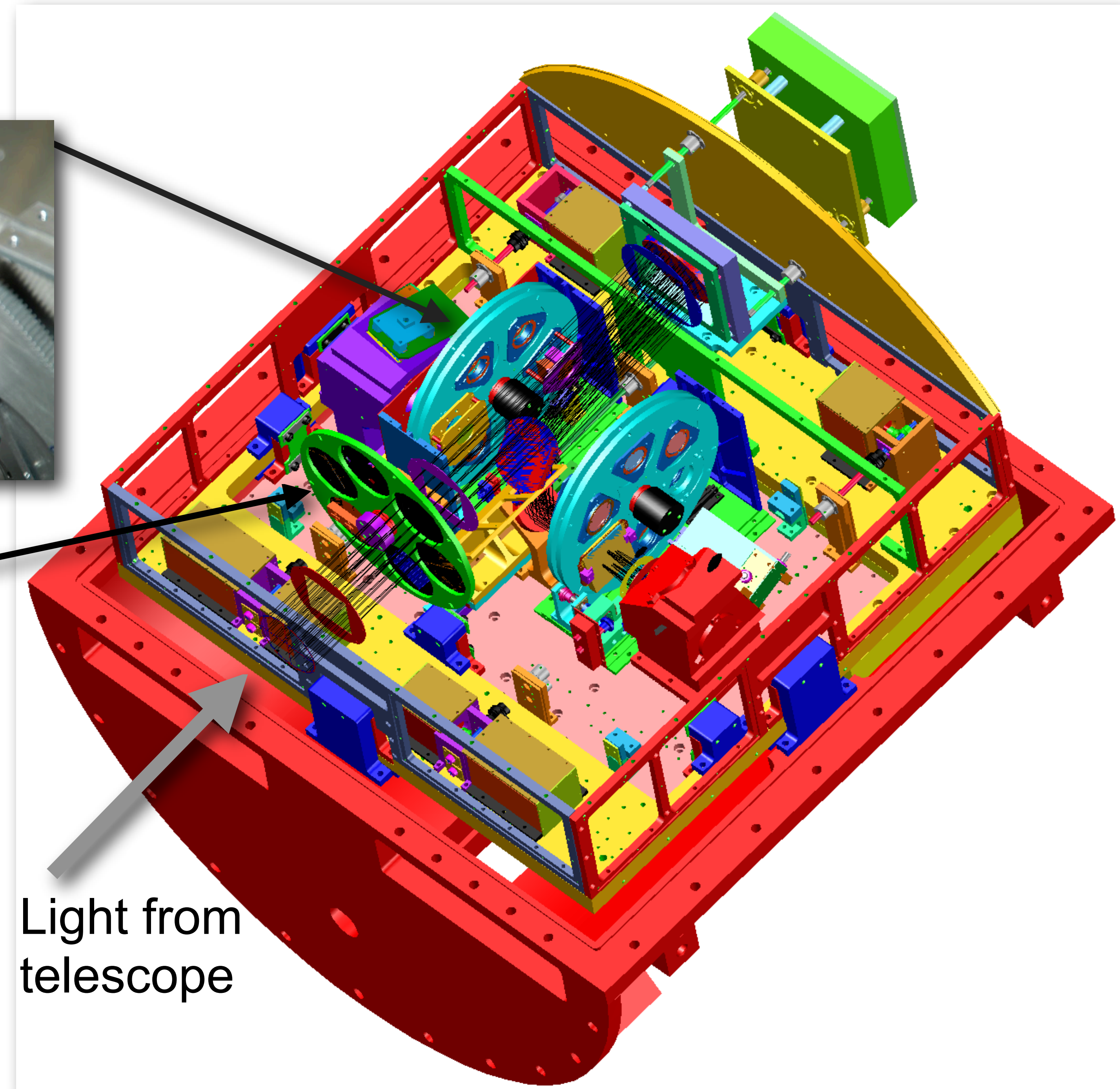

FORCAST grism design overview: history

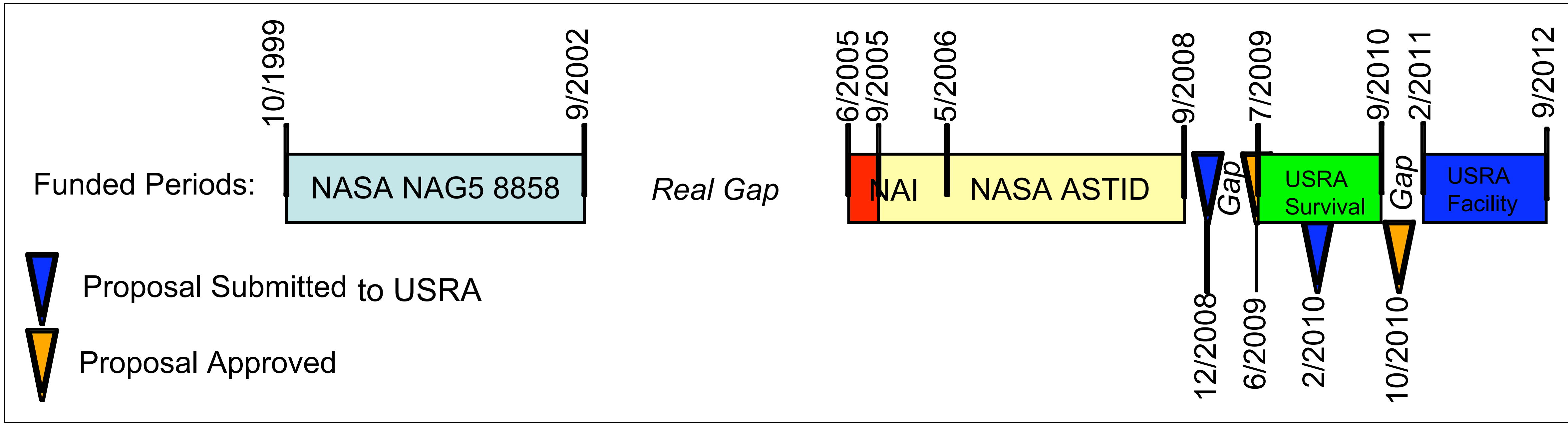

2005-2008: Grism fabrication and initial lab testing (funded by ASTID, K. Ennico, PI)
2009: Proposal to USRA/NASA for funding --> facility-class grism mode
2009-2010: "Survival" funding keeps project alive
2011: USRA/NASA funding for facility-class mode (L. Keller, PI)
2011: Re-install and test all grisms in FORCAST, flight configuration established
2012: In-flight testing and commissioning, late spring - early summer
2012: Offered as a shared-risk observing mode during SOFIA Cycle 1

Cycle 1 FORCAST grism observing modes

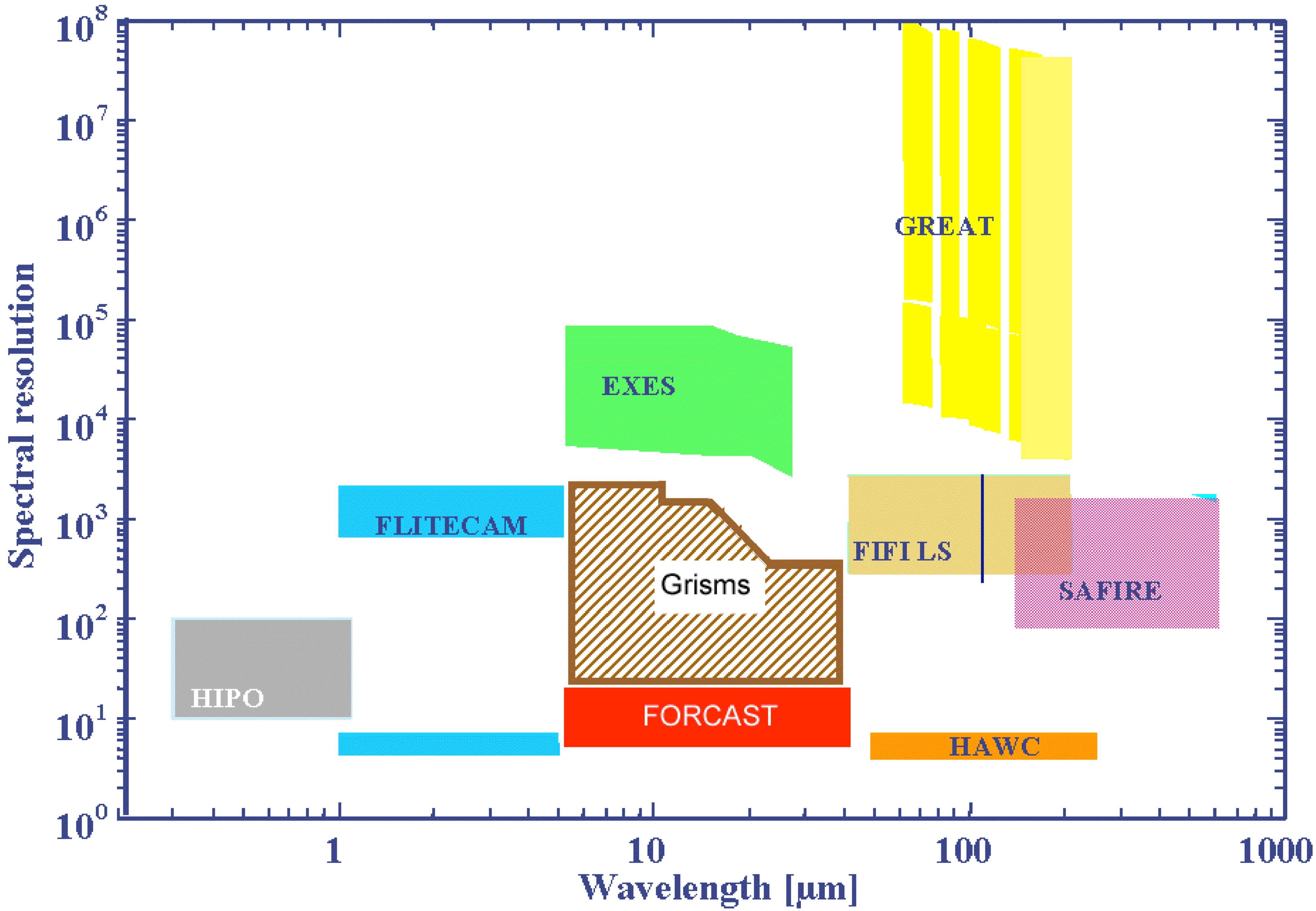

Cycle 1 FORCAST grism observing modes

Grism	Wavelength	Slit	Resolving Power
Long Slit Spectroscopy in the Short Wavelength Camera			
G1	4.7-7.8 μm	2.4”x192”	200
		4.7” x192”	100
G3	8.4-13.7 μm	2.4” x192”	300
		4.7” x192”	150
Cross Dispersed Spectroscopy in the Short Wavelength Camera			
G2xG1	4.7-7.8 μm	2.4”x11.25”	1200
G4xG3	8.4-13.7 μm	2.4”x11.25”	800
Long Slit Spectroscopy in the Long Wavelength Camera			
G5	17.6-27.7μm	2.4”x192”	140
		4.7” x192”	70
G6	28.7-37.1μm	2.4” x192”	220
		4.7” x192”	110

FORCAST grism spectroscopy compared to *Spitzer* IRS

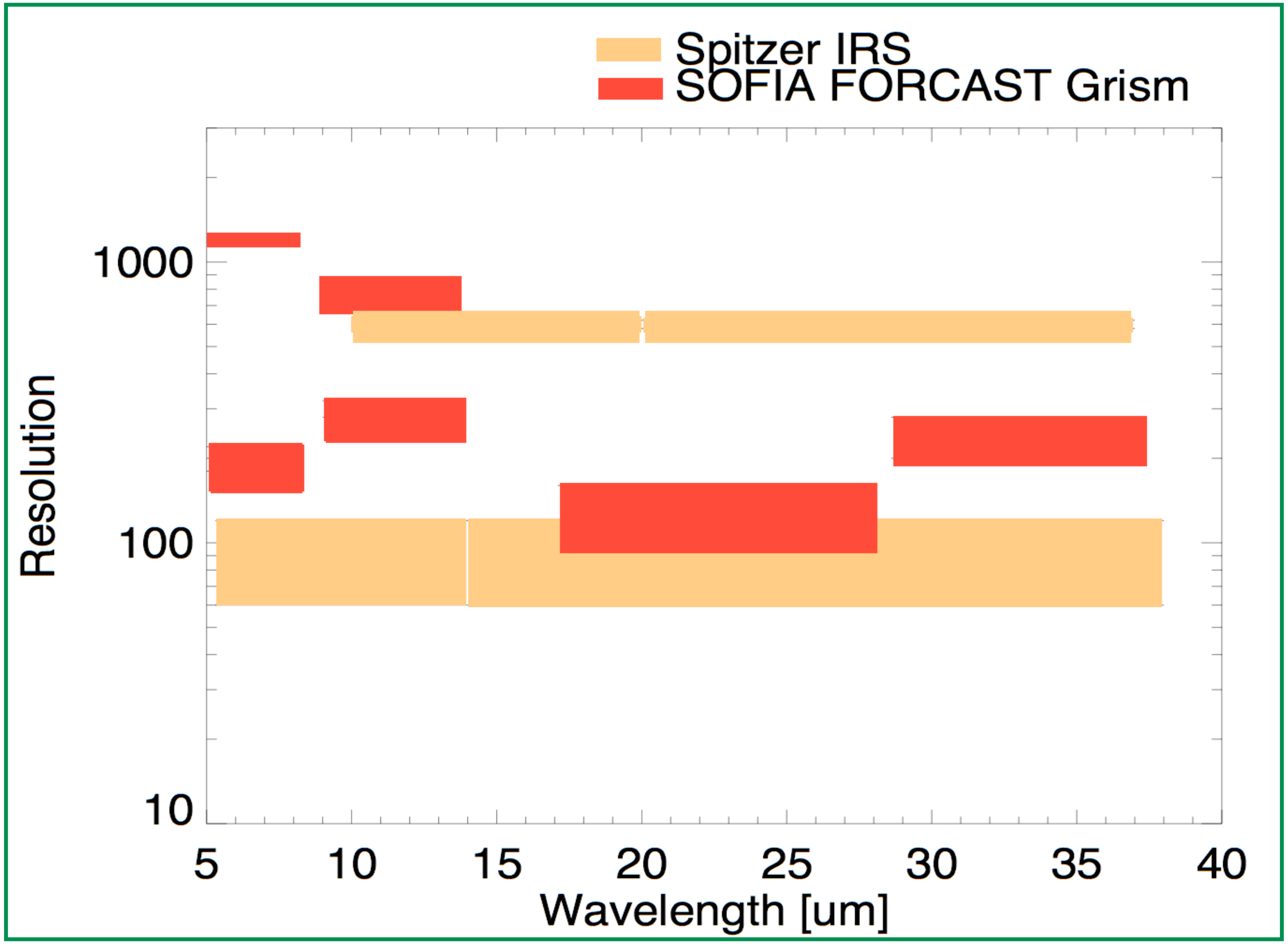

Cycle 1 FORCAST grism observing modes

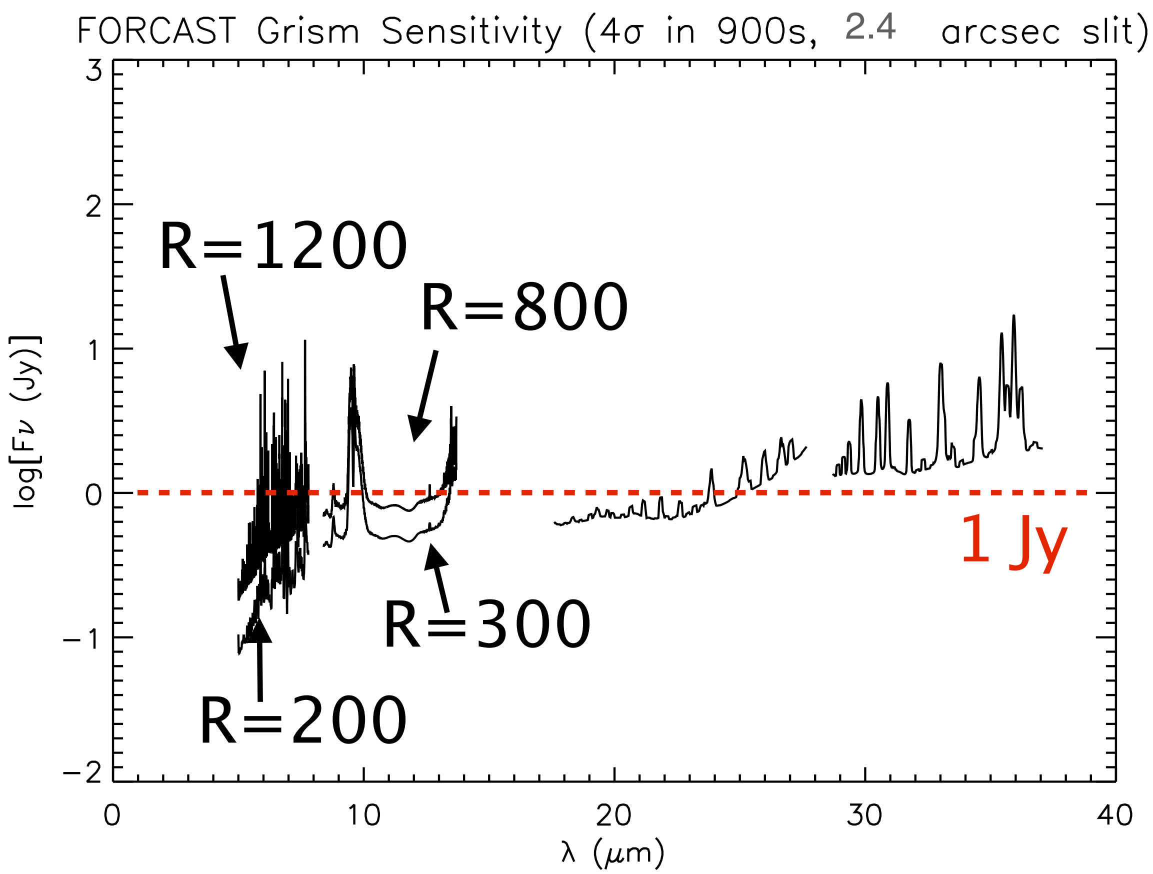

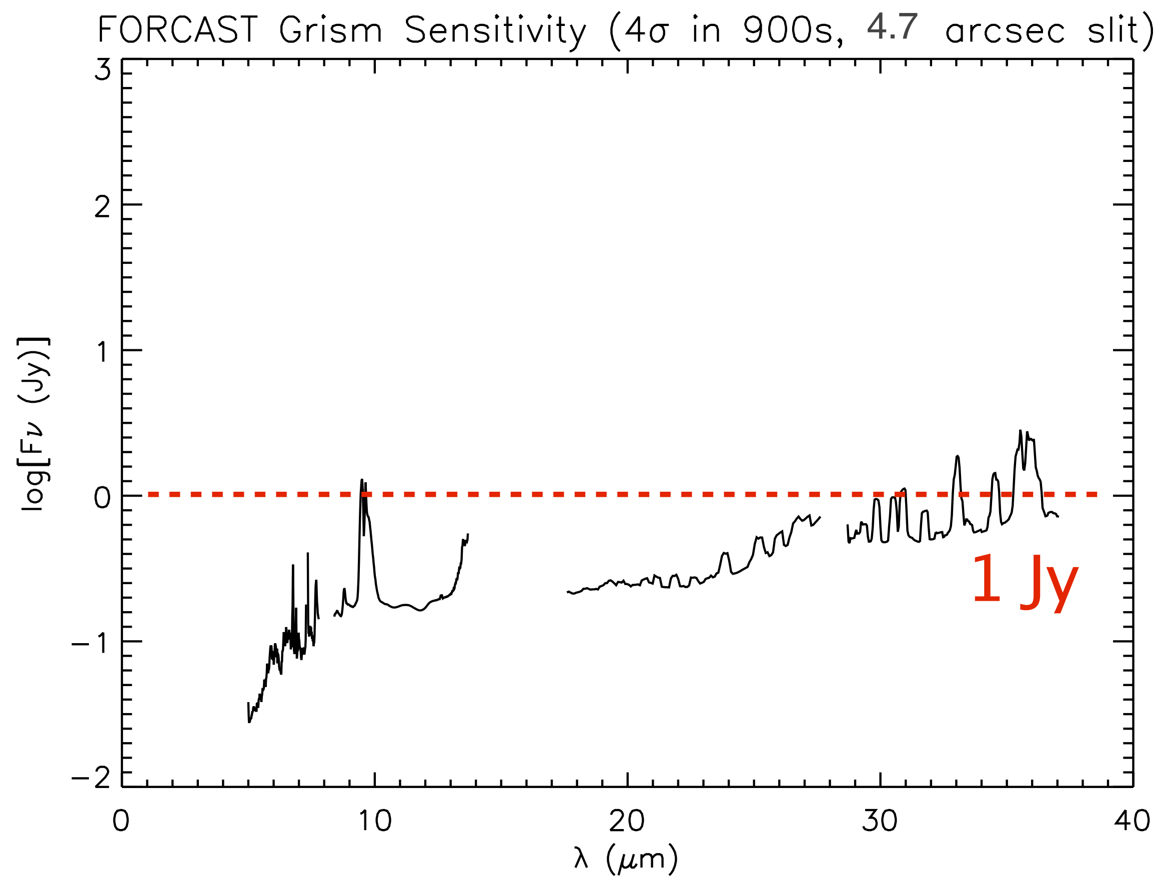

Estimated Point Source Sensitivity
(Assumed 7.1 μm PWV; 41,000 ft altitude; 45º telescope elevation)

Sample data

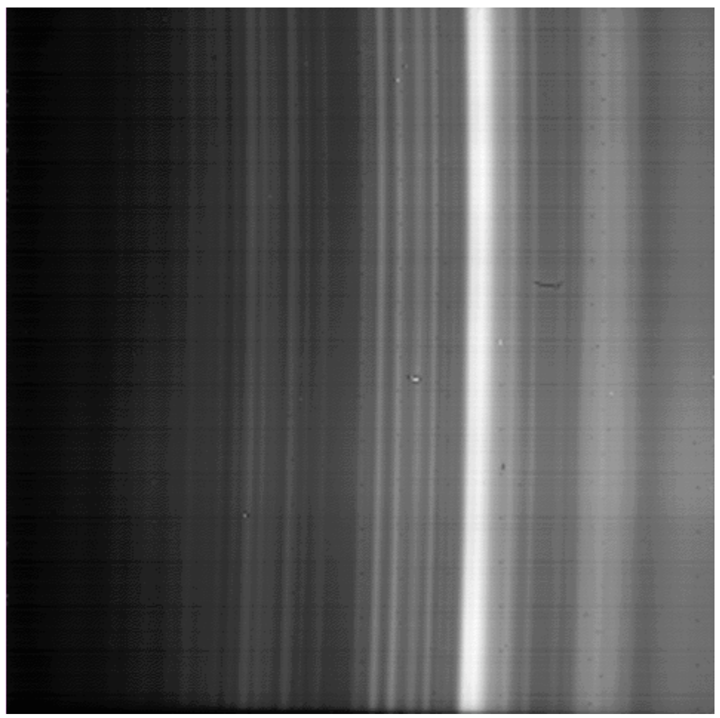

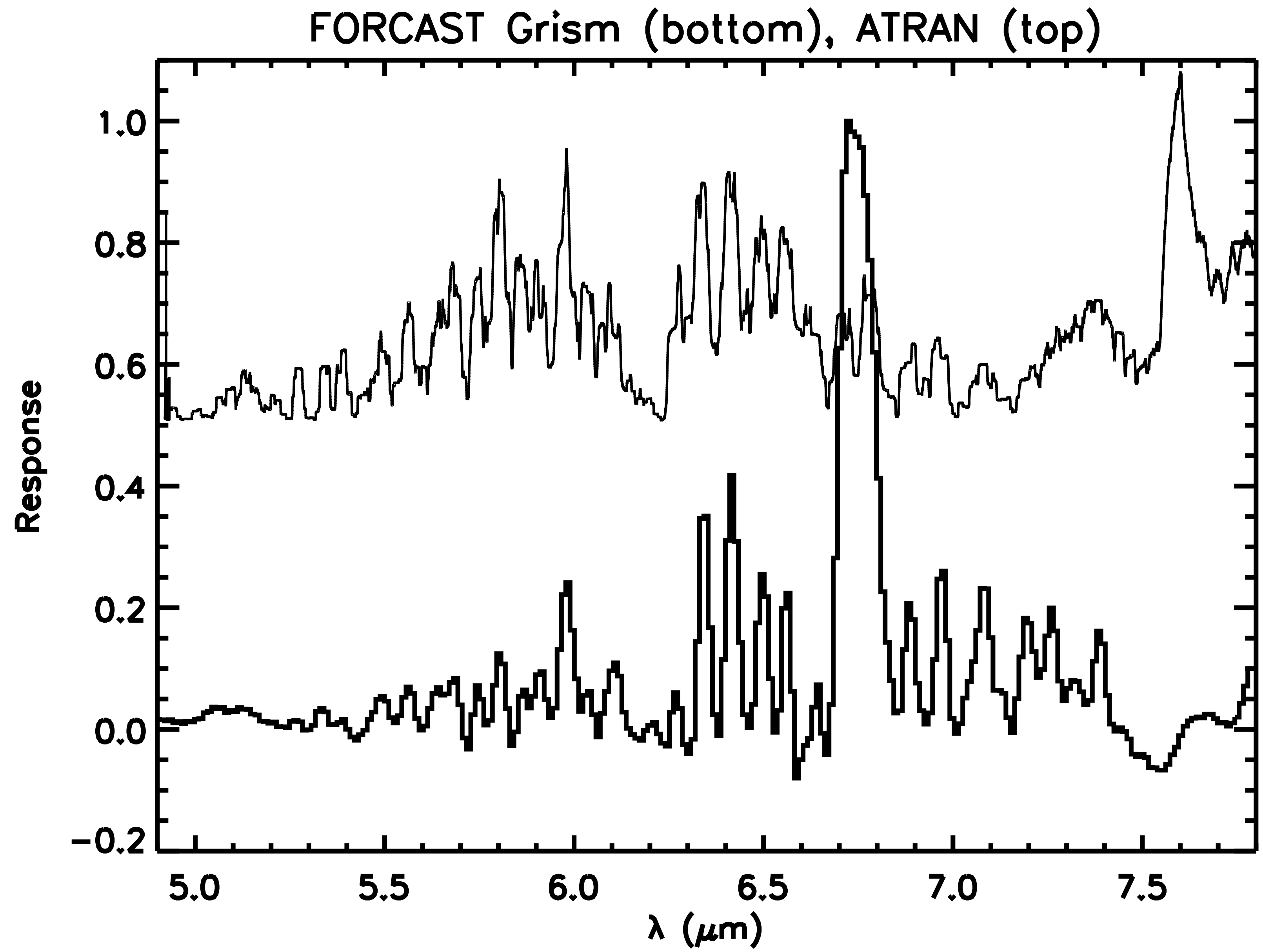

Lab test spectrum for Grism 1 (in FORCAST): 4.9-7.8 μm,
R=200 (Water vapor in emission against a 77K background)

Sample data

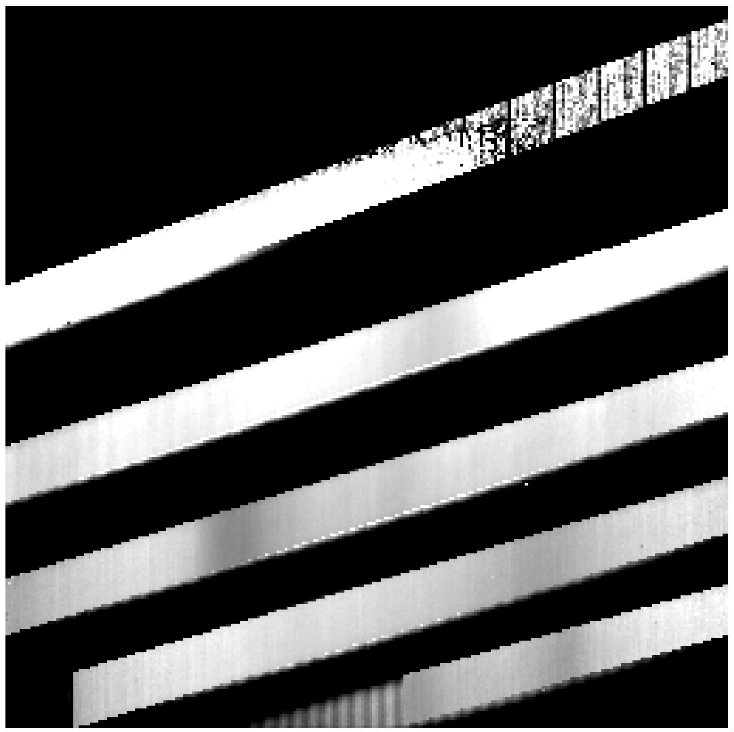

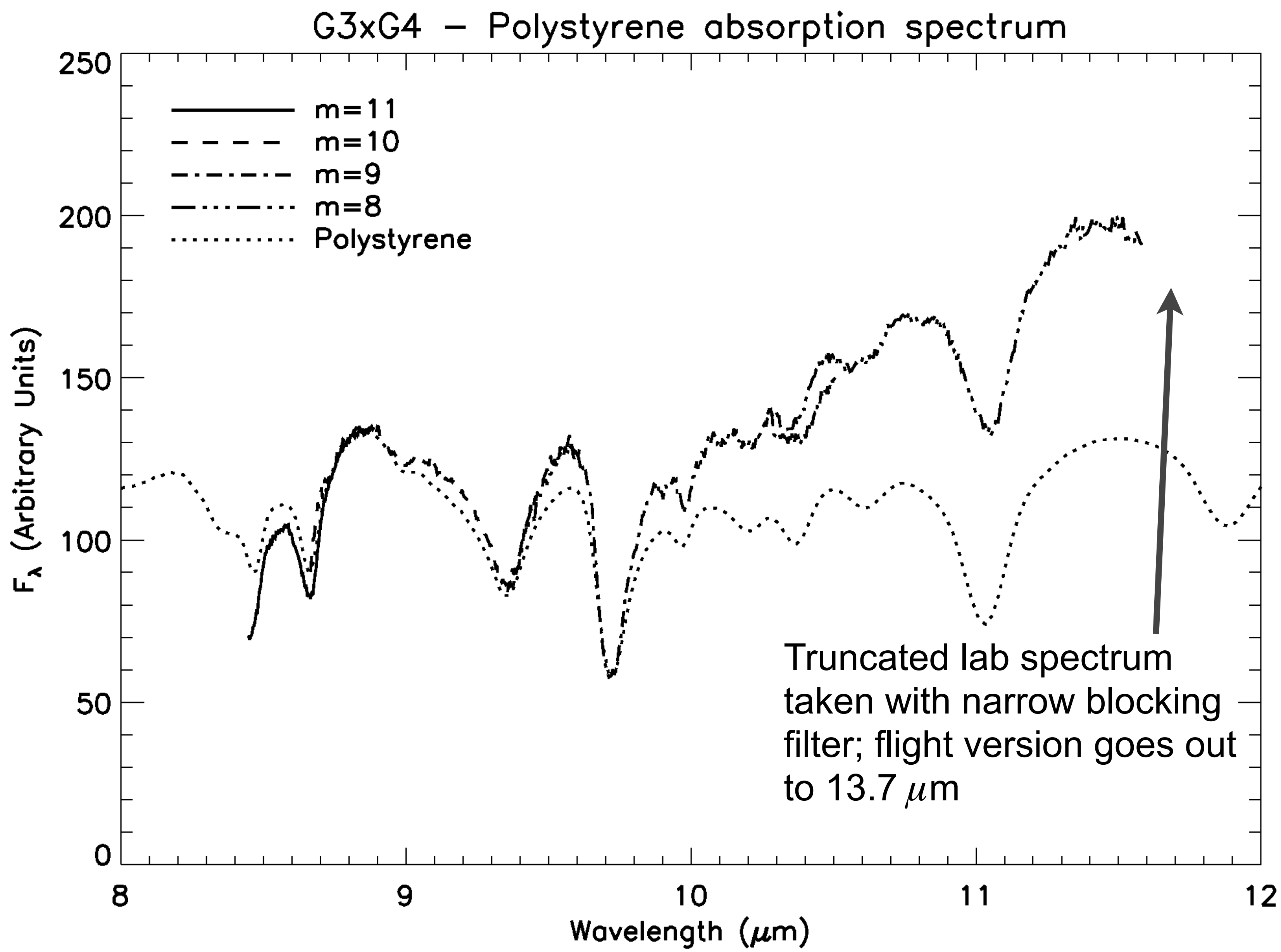

Lab test spectrum for Grism 3 (in FORCAST): 8.4 - 13.7 μm, R=300 (300 K continuum emission through polystyrene)

Sample data

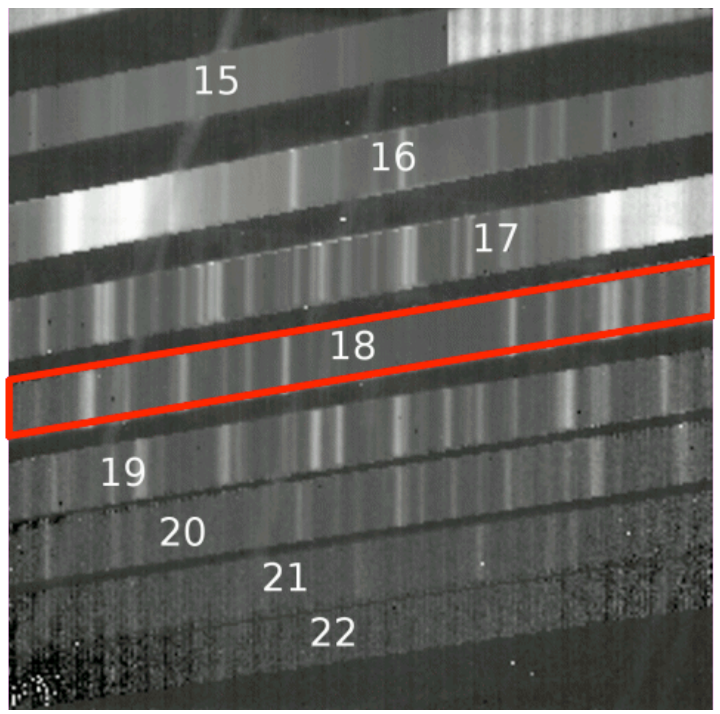

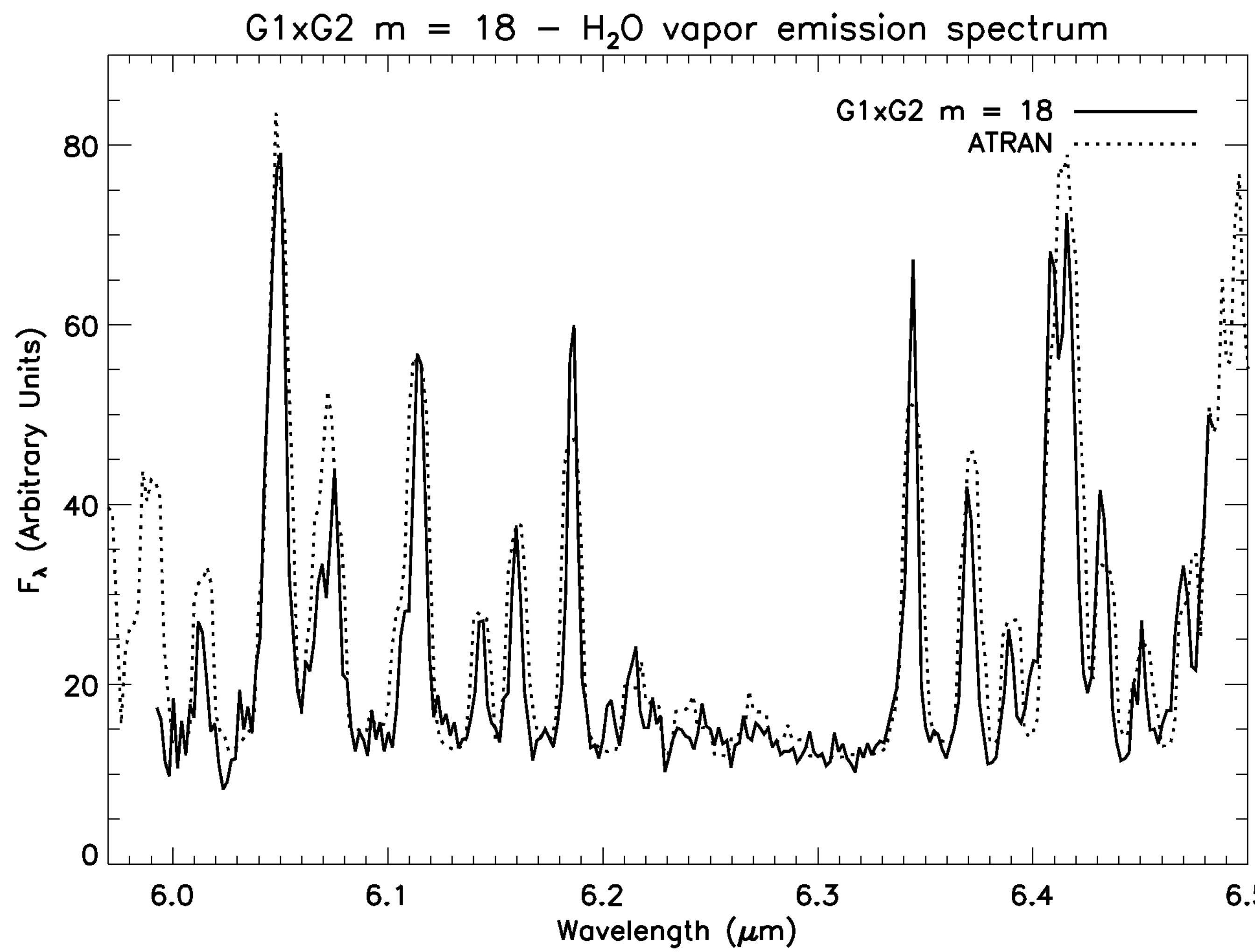

Lab test spectrum for Grism 1 (in FORCAST): 4.9-7.8 μm, R=1200 (Water vapor in emission against a 77K background)

Data artifacts

- Interference fringes removed in ***flatfield*** and ***defringe*** pipeline steps

- "jailbar" array pattern noise removed in ***jailbar*** pipeline step

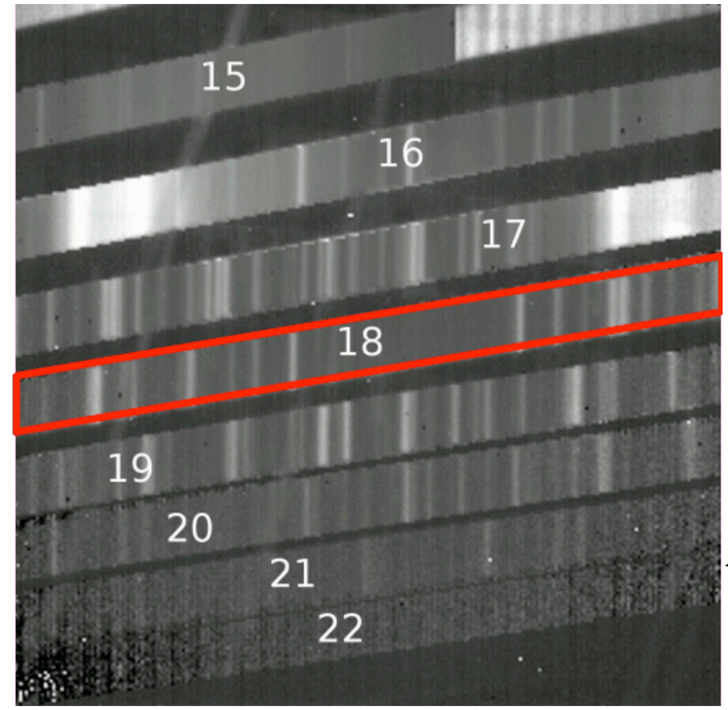

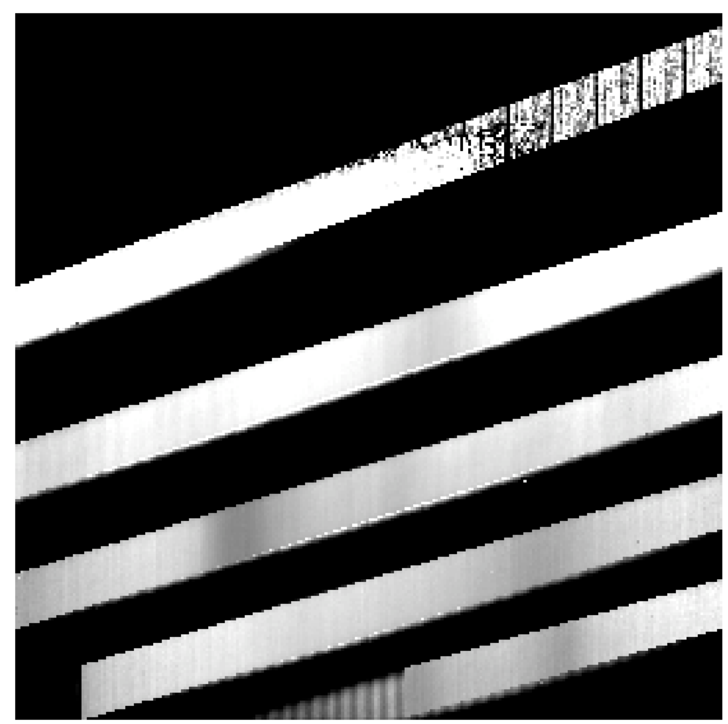

Observation set-up: long slit source acquisition

Keep in mind:

- There is no slit viewer; but we can image through the slits
- Nod or chop axis must be aligned with the slit
- Dithering along slit only; will attenuate “jailbars”
- Both symmetric and asymmetric chop possible along slit
- Telescope line-of-sight resets will rotate field, NOT slit

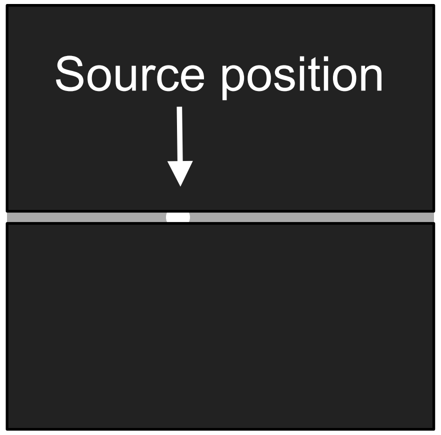

NPC with nod off slit
(Nod-Perpendicular-to-Chop)

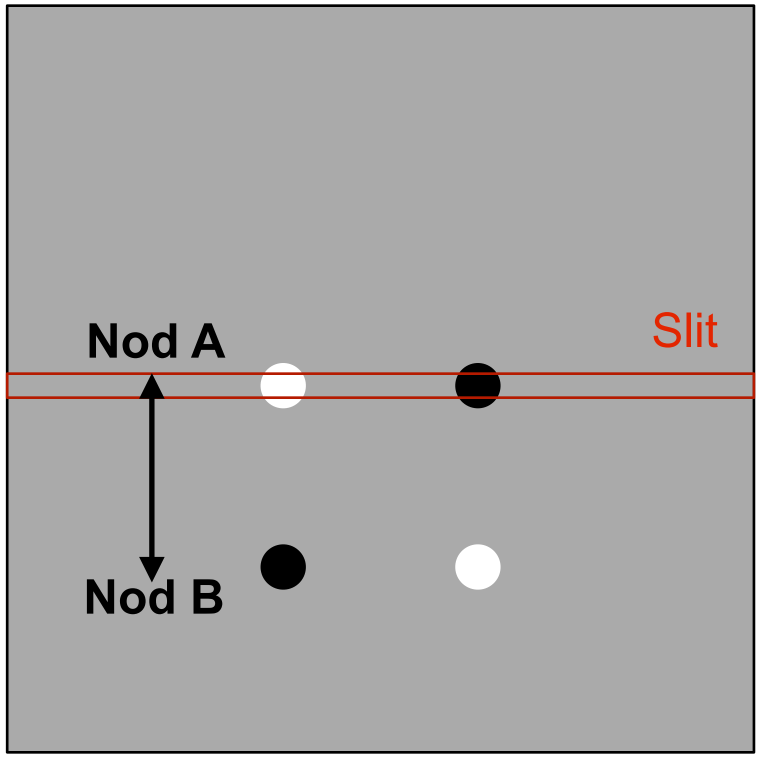

NPC with nod along slit
(Nod-Perpendicular-to-Chop)

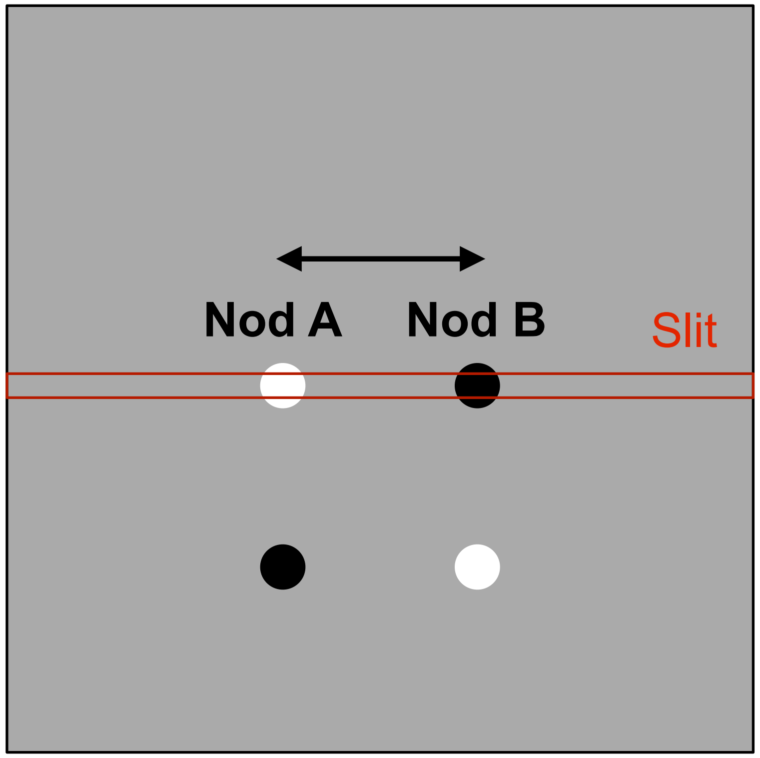

NMC with dither along slit
(Nod-Match-Chop)

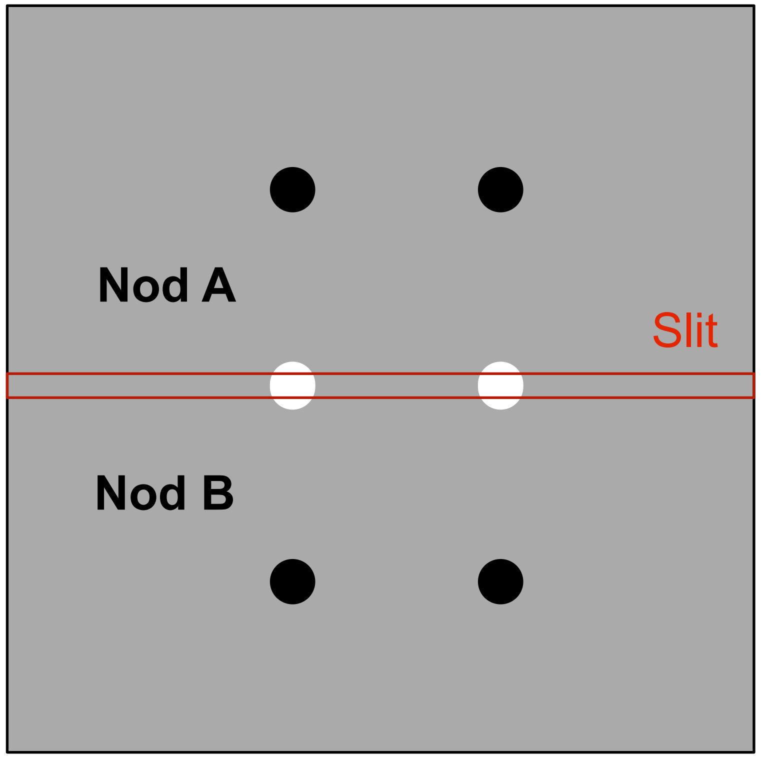

Observation set-up: short slit source acquisition

Keep in mind:

- There is no slit viewer, but we can image through the slits
- Most sources will be too large for nodding along slit
- Limited dithering (11.25” slit length), will not remove “jailbars” (parallel to short slit)
- Slit length allows asymmetric chop only
- Telescope line-of-sight resets will rotate field, NOT slit

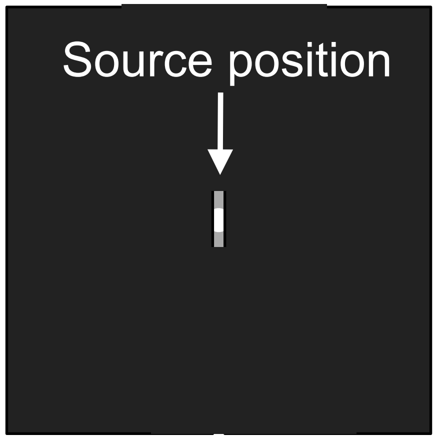

NPC with nod off slit
(Nod-Perpendicular-to-Chop)

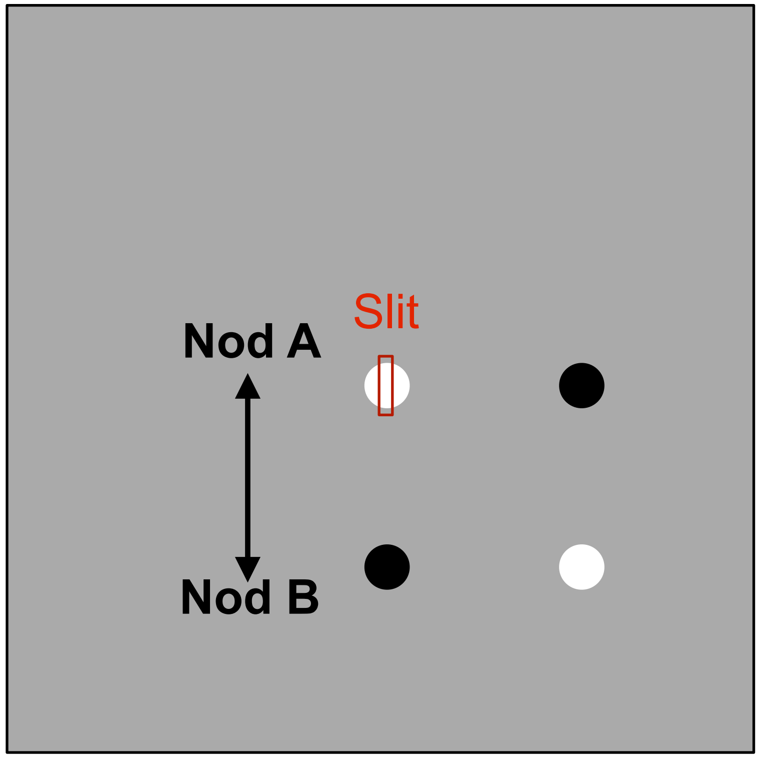

NMC with nod along slit direction
(Nod-Match-Chop)

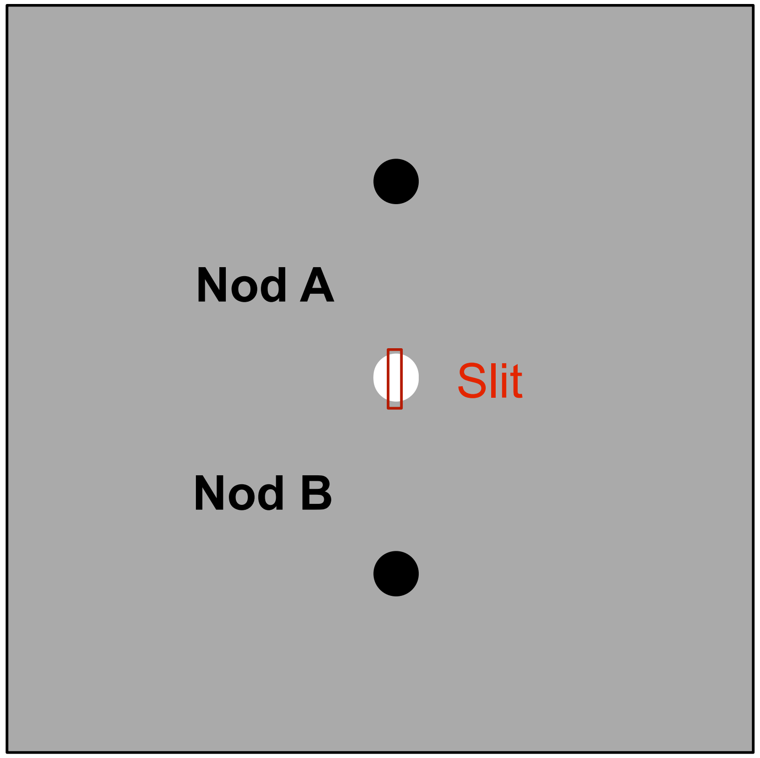

Pointed observations & mapping in extended sources

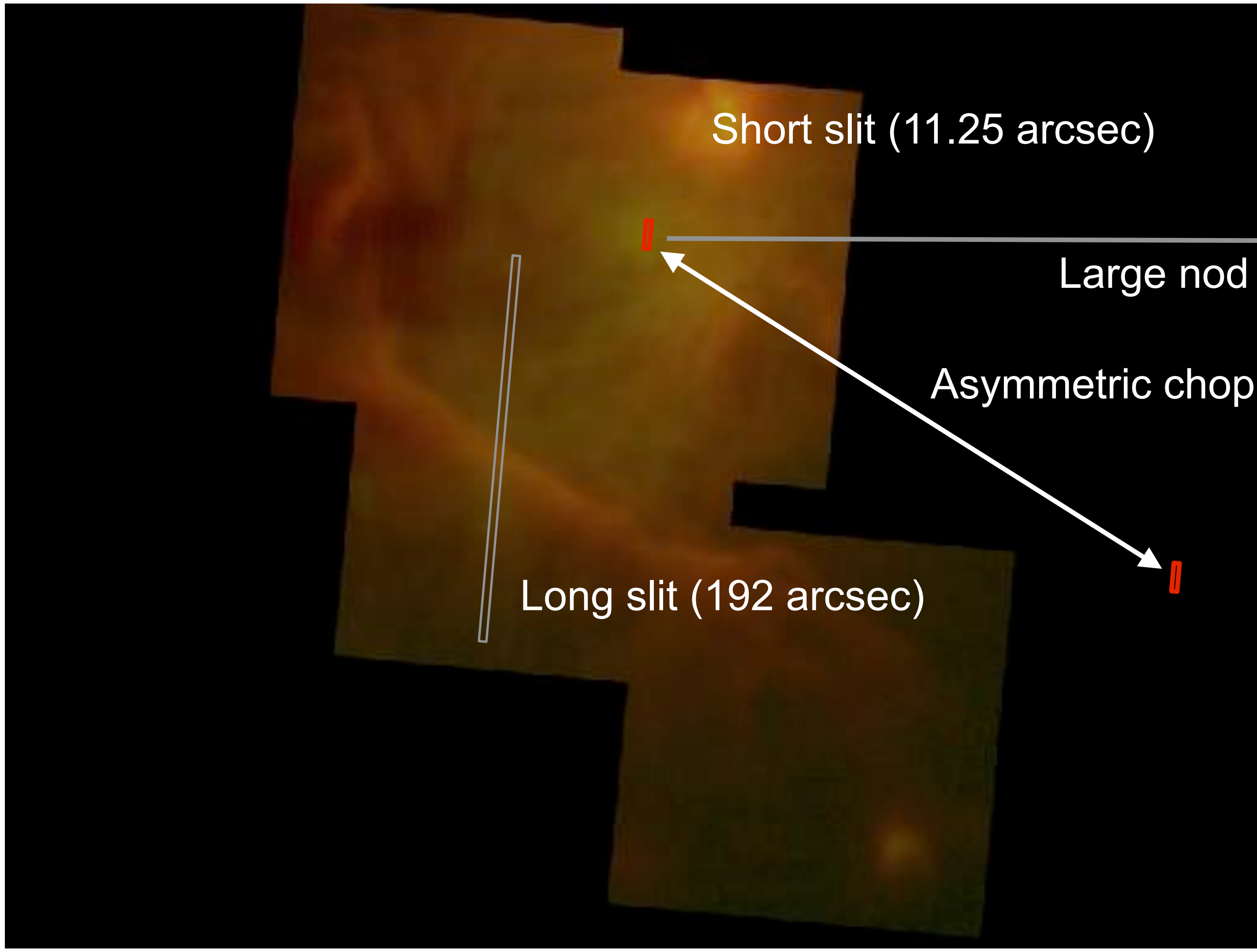

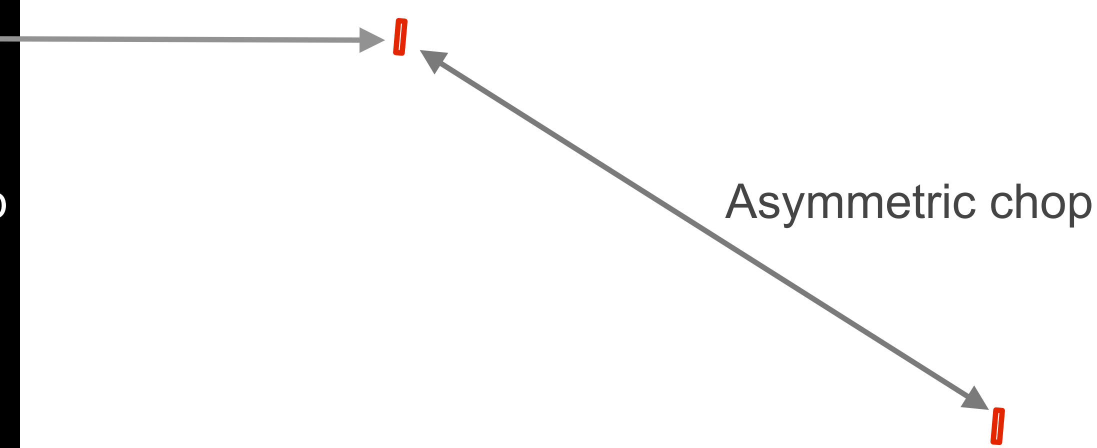

Large HII region example C2NC2 mode

Galaxy example NMC

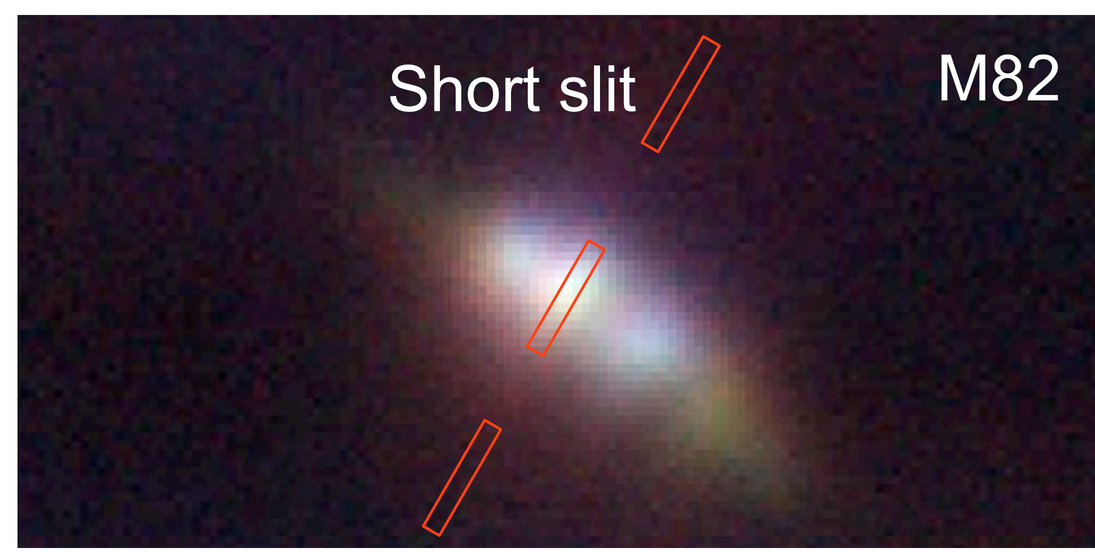

NOTE: Slit scan possible, details under construction

Data reduction steps

Imaging pipeline:

- ***clean***: remove bad pixels
- ***linearize***: detector non-linearity correction
- ***flatfield***: may also remove interference fringes
- ***stack***: background subtraction using chop/nod sets
- ***jailbar***: remove pattern noise

Additional pipeline steps for grism spectroscopy

- ***spectral extraction***: (optimal or sum columns)
- ***defringe***: if needed after flatfield correction (e.g. low S/N)
- ***wavecal***: apply pre-determined polynomial fit to telluric/nebular lines
- ***telluric****: using observed telluric spectra, pwv data, and ATRAN models
- ***fluxcal***: using observed spectra of flux calibration stars
- ***save***: extracted and calibrated spectra, any specified intermediate data set

* Telluric spectrum removal may not always be optimized as an automatic pipeline step. This will depend on the frequency and quality of telluric standard star observations during the flight.

Flux calibration plan

S: Source spectrum
C: Calibrator spectrum
T: Transmission spectrum
I: Instrument spectrum
A: Atmosphere spectrum

$$S_{true} = \frac{C_{true}}{C_{obs}} S_{obs}$$

$$\frac{C_{true}}{C_{obs}} = T(\lambda) \qquad T(\lambda) = I(\lambda)A(\lambda)$$

$$A(\lambda) = A_{H_2O} A_{CO_2} A_{O_3} A_{Ev}$$

- Spectrophotometric calibration will use observations of stars interleaved with primary source observations. Optimal would be airmass-matched standard star observations for each program source, but this may not always be possible in a given flight plan. Goal is observations of calibrators at high & low airmass both early and late in the flights, plus additional calibrator observations during the flight.

- Wavelength calibration is a third-order polynomial fit to telluric (and/or nebular lines). Predetermined wavecal applied in pipeline reduction.

Additional observation planning strategies & challenges

- No dual-channel observations in Cycle 1, but using opposite FORCAST channel for target acquisition and verification during integration is possible. Otherwise imaging through the slit (no slit viewer).

- Reminder: the slit position angles are fixed (cannot rotate), but the field WILL rotate a few degrees per line-of-sight "rewind" on a cadence that depends on the aircraft heading (e.g. position of source in the sky). Observations that require a specific slit position angle will depend on flight planning.

- As a precaution, two long slit widths (2.4" and 4.7") are available. Wider slit will help with slit losses created by image instabilities. Short slit is 2.4" since it is used for modes with high spectral resolving power.

Thanks and happy data taking...

Questions & Comments: Luke Keller (lkeller@ithaca.edu)

Appendix A: FORCAST Grism design and development publications

1. Keller, et al. "Protostars and Planets V," Proceedings, No. 1286., p.8481. (2005), Hawaii, October 2005.
2. Ennico, et. al. AAS Meeting 207, #129.02; Vol. 37, p.1376 (2005), Washington, DC, January 2006.
3. Mar et al, SPIE 6269.184-192 (2006), Orlando, Florida, May 2006.
4. Ennico et al, SPIE 6269.57-66 (2006), Orlando, Florida, May 2006.
5. Adams, et al. SPIE 6269.34-44 (2006), Orlando, Florida, May 2006.
6. Keller, et al. "SOFIA 2020 Vision Meeting", Caltech, December 2007.
7. Ennico, et al. AAS Meeting 211, #11.14; Vol. 39, p.746 (2007), UT Austin, January 2008.
8. Deen, et al. SPIE 7014:7014-23 (2008), Marseilles, France, June 2008
9. Keller et al. SPIE, San Diego, CA, USA, June 2010
10. Deen et al. SPIE, San Diego, CA, USA, June 2010

Appendix B: Science motivation for FORCAST grism spectroscopy

One of the great strengths of SOFIA is the breadth of capabilities it offers including high resolution spectroscopy--over a broad range of wavelength--that *complement the capabilities of recent, current, and future space infrared observatories.* Examples of science enabled by FORCAST grism spectroscopy:

The evolution of refractory grains from their formation to their incorporation in protoplanetary bodies and solar system bodies (most notably comets)

Spatial distribution and physical characteristics of large molecules like the polycyclic aromatic hydrocarbons (PAH's) in Galaxtic and extra-galactic ISM, protoplanetary disks (the brightest disks tend to the be closer and more extended)

The FORCAST grism modes, together with FIFI-LS, can study interstellar ices in both absorption and emission to give us a handle on the icy material while ALMA and EXES examine the gaseous side of the interplay between the two states. In protoplanetary disks, the information provided by grism spectroscopy, in concert with the longer wavelength instruments, will allow us to follow the chemical state of the icy solid material as these systems evolve and, through studies of comets, to observe this material within more mature planetary disks.

FORCAST grism spectroscopy exemplifies the utility of SOFIA in bridging other infrared observatories and offering higher spatial and spectral resolution than current infrared space observatories. Hershel, for example, does not cover the FORCAST wavelength range for imaging or spectroscopy and JWST will not offer imaging or spectroscopy beyond 28 mm. FORCAST grism spectroscopy will span this gap enabling more and richer scientific investigations.

Circumstellar dust

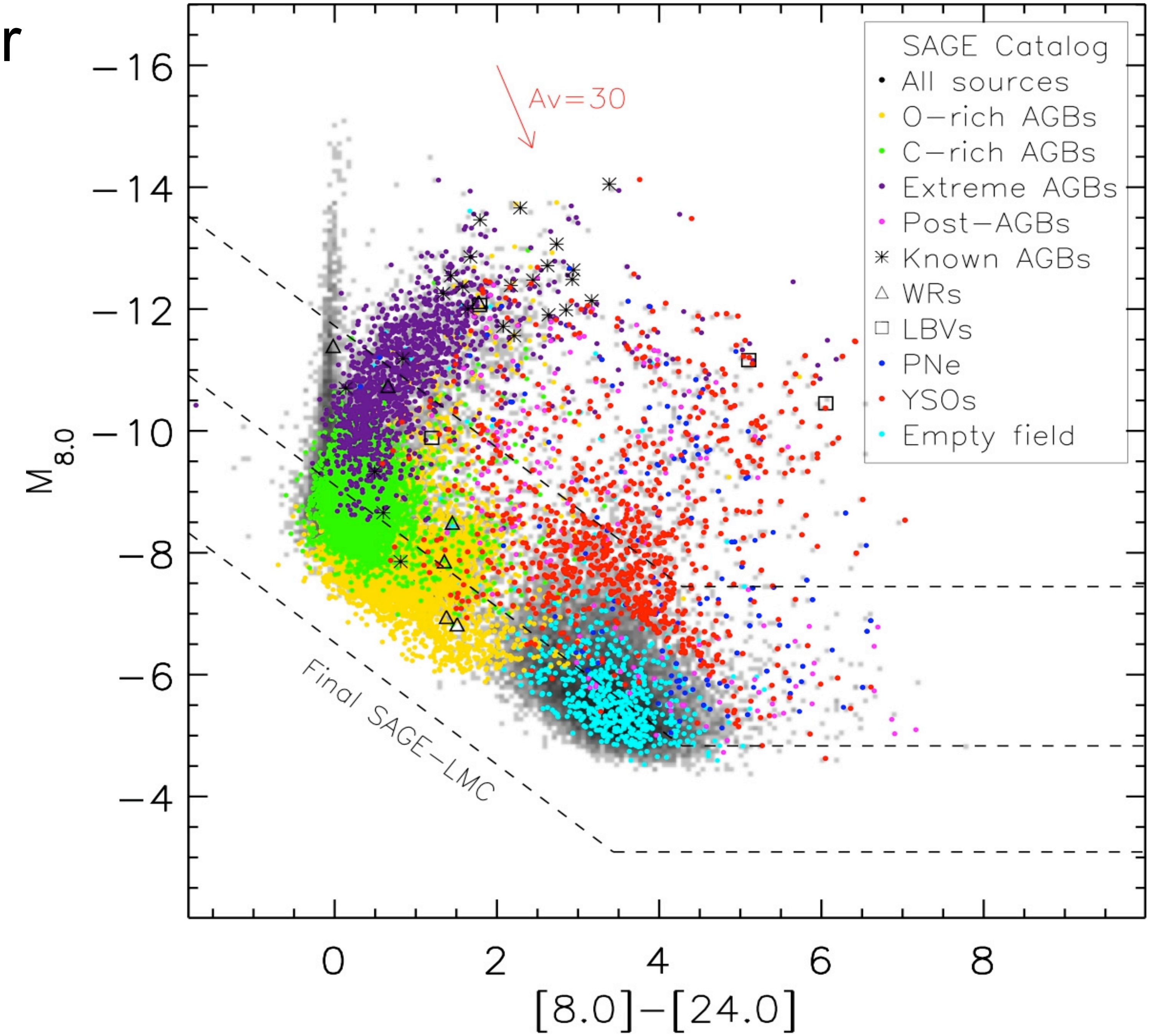

Figure 3-6. *Infrared color-magnitude diagram of stars in the nearby galaxy, the Large Magellanic Cloud, obtained by the SAGE Spitzer Legacy Program (Blum et al. 2006; Meixner et al. 2006). Different classes of objects – indicated by different color symbols –segregate into different parts of this diagram due to differences in dust composition and spectral characteristics, while their distribution reflects intrinsic variations in mass-loss rates. The GAIA mission will provide accurate distances for stars in the Milky Way and this will enable similar color-magnitude diagrams for our own galaxy. The dashed lines indicate the SAGE photometry limits for the LMC and the predicted sensitivity limits (10 σ in 900 sec) for FORCAST in the GRISM mode for these types of objects at 3 and 10 kpc, respectively, in the Milky Way. Figure is courtesy of M. Sewilo & SAGE team.*

Life cycle of dust

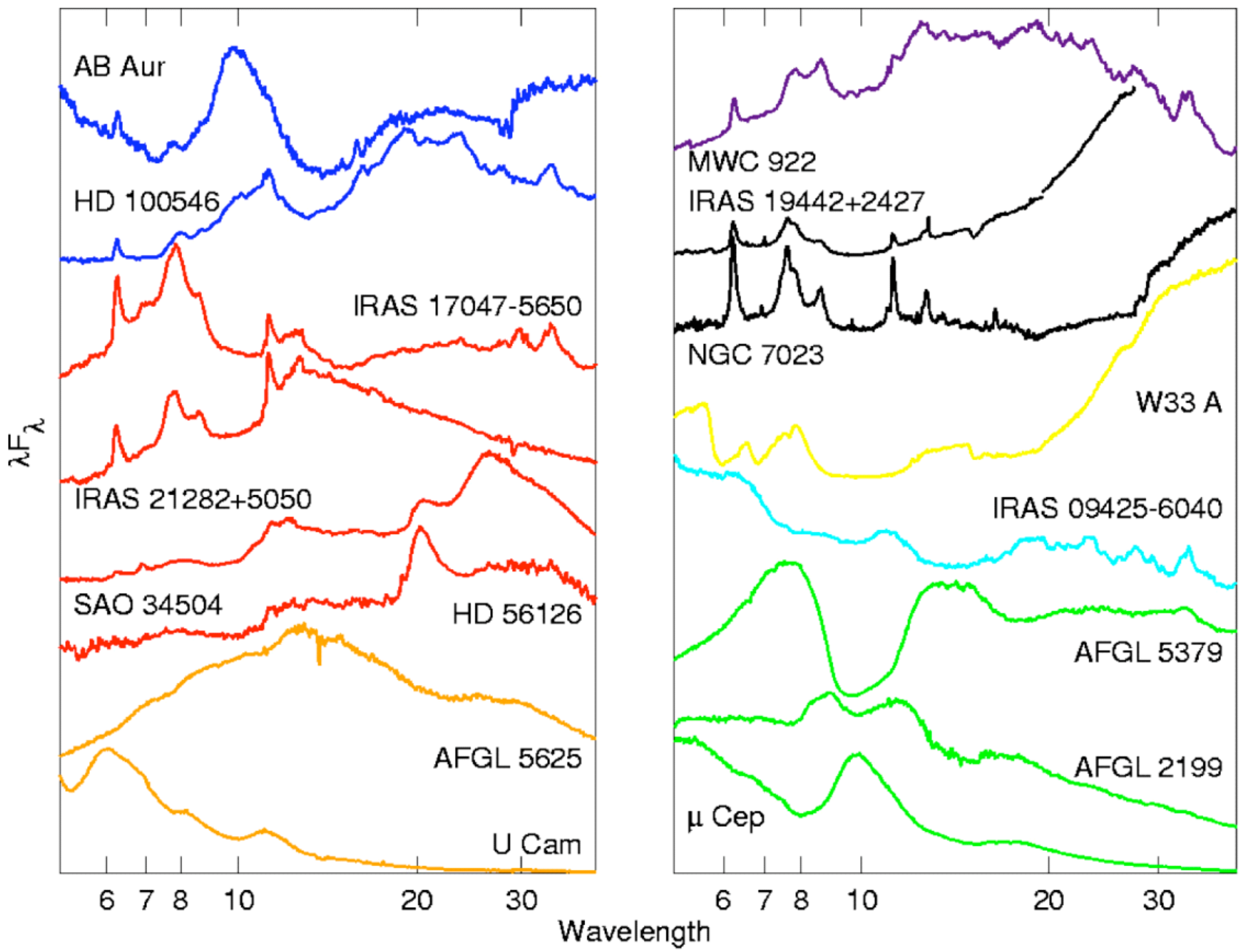

Figure 3-5. *The rich and spectrally diverse stardust revealed by ISO and Spitzer requires systematic study. A selection of ISO SWS spectra of a variety of objects shown here illustrates the rich spectral diversity of the dusty Universe . Key: dark blue: Herbig AeBe; red: post-AGB and PNe; orange: C-rich AGB; green: O-rich AGB; light blue: mixed chemistry AGB; yellow: deeply embedded YSO; black: HII region/reflection nebula; purple: mixed chemistry post-AGB.*

ISM: PDR environmental characteristics

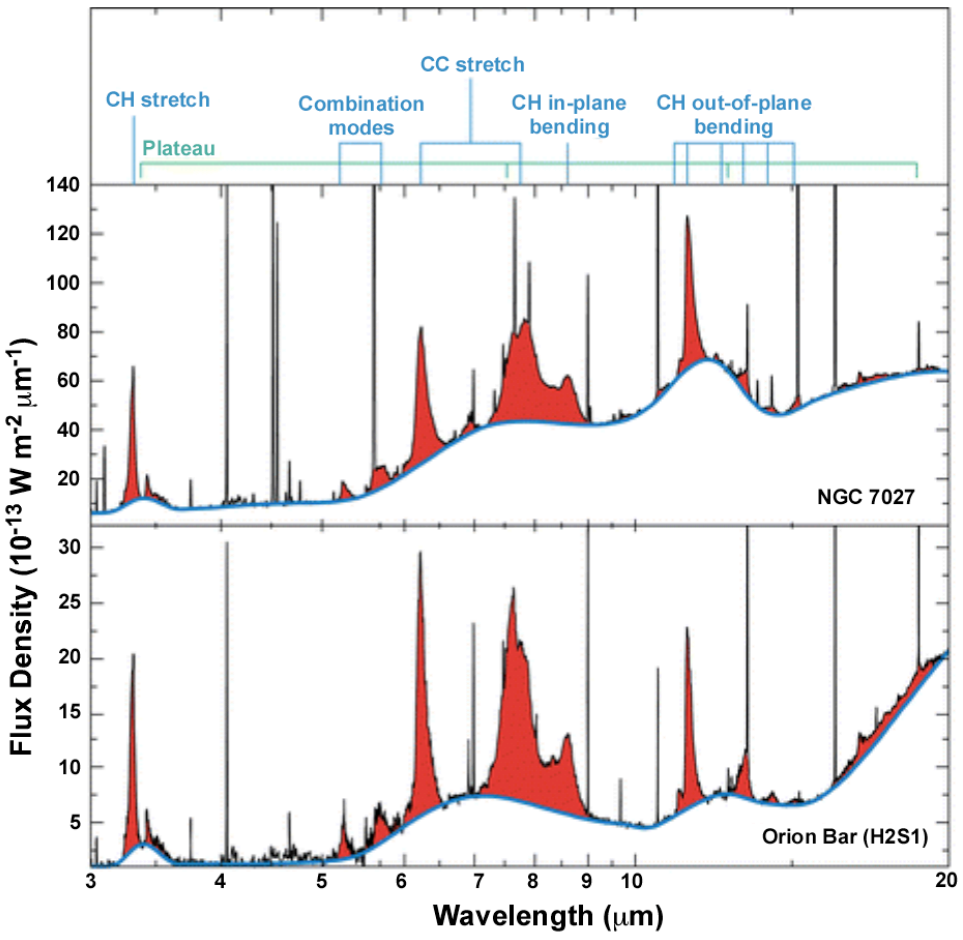

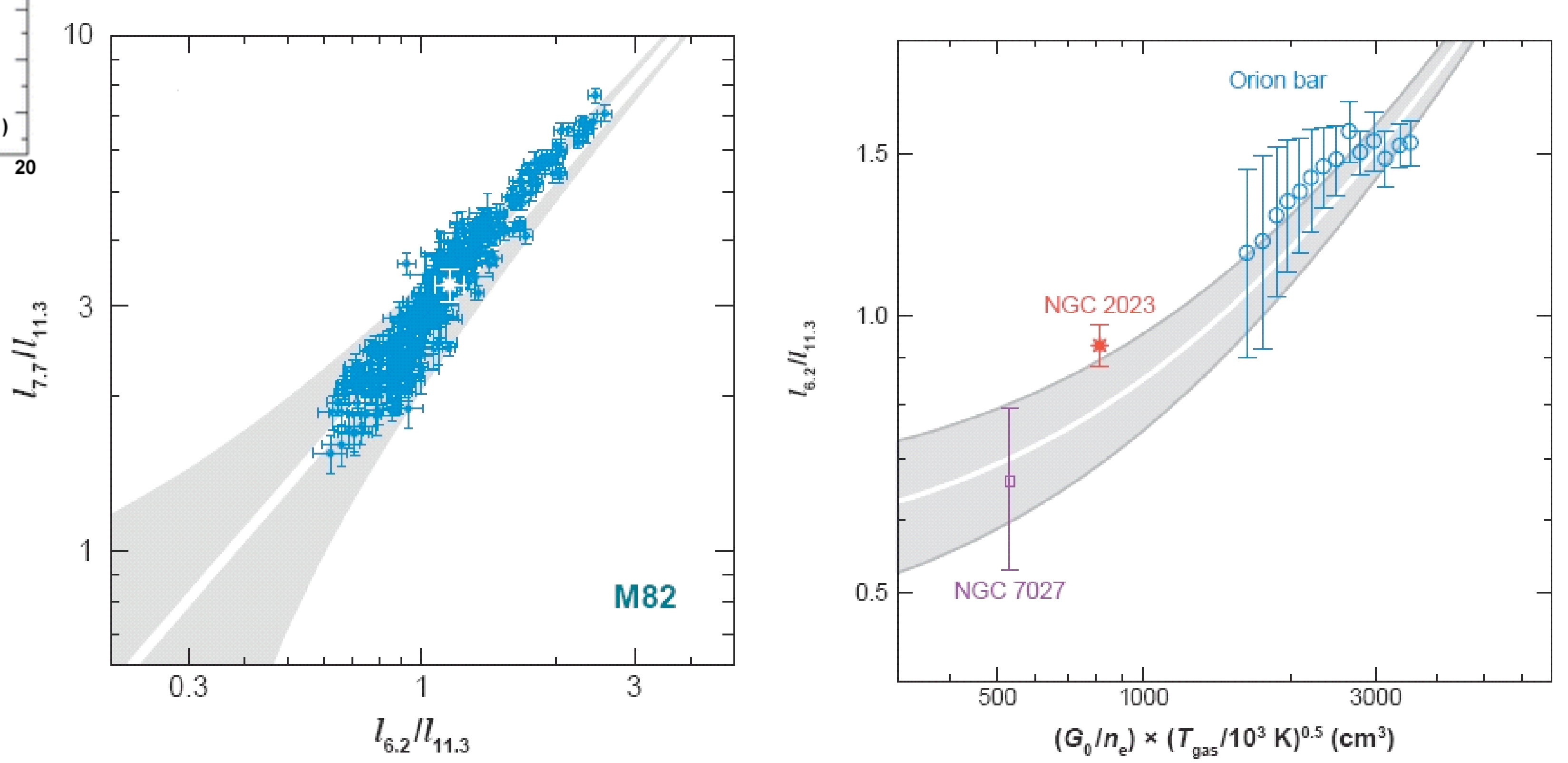

Figure 3-4. *Left panel: Variations in the relative strength of the 6.2, 7.7, and 11.3 μm PAH bands observed in the starburst galaxy, M82 (Galliano et al., 2008). As these data illustrate, the 6.2 and 7.7 μm bands – due to PAH cations – vary relative to the 11.3 μm band – due to neutral PAHs – by a factor of 4 in this data set. Similar variations are observed in many other sources. Right panel: The observed ratio of the 6.2 to 11.3 μm band – a measure of the ionization balance of PAHs is related to the physical conditions in a few well-studied PDRs through the ionization parameter, $G_oT^{1/2}/n_e$, a measure of the ionization rate over the recombination rate (Galliano et al. 2008).*

Solar system: comet chemistry and mineralogy

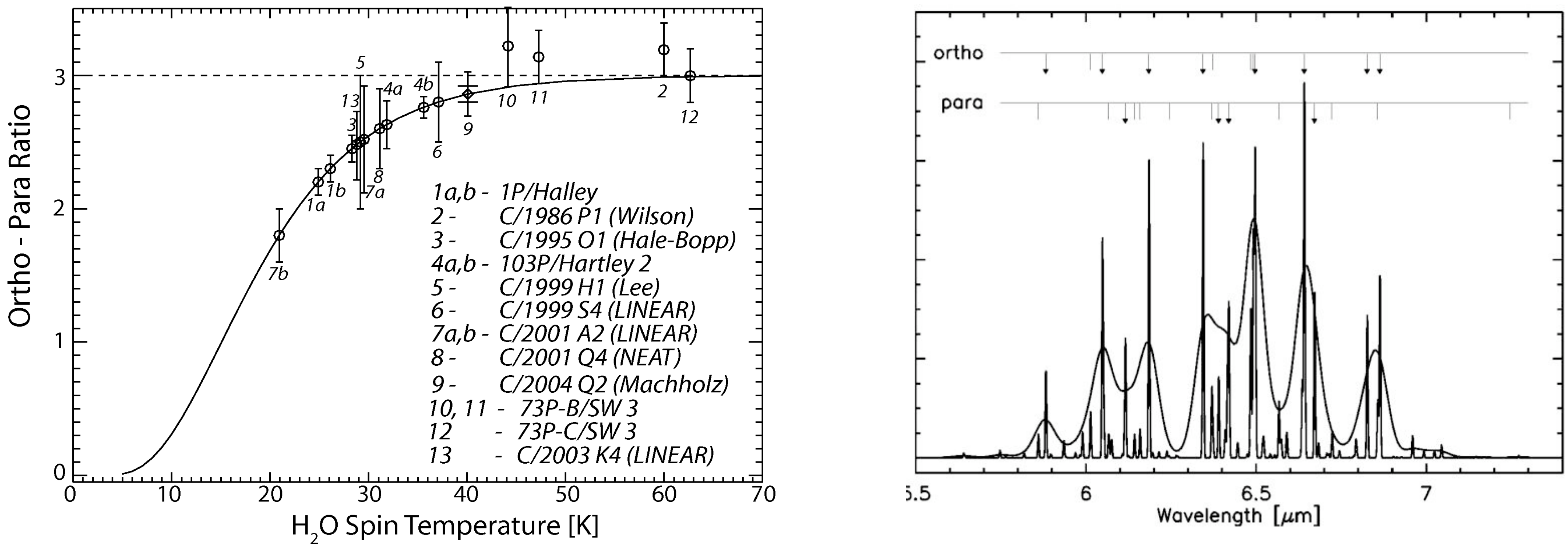

Figure 5-3. *(Left): Ortho-para ratios for H_2O in comets (Bonev et al. 2007) placed on a theoretical curve connecting them to the corresponding formation temperature. (Right): The 6.5 µm H_2O band in comet K4, both fully resolved and also convolved to the resolution of Spitzer (Woodward et al. 2007). Ortho and para lines are indicated. EXES on SOFIA would provide major improvement in the detection limits by resolving lines of each spin isomer, and eliminating spectral confusion from interloping lines.*

Solar system: planetary atmospheres

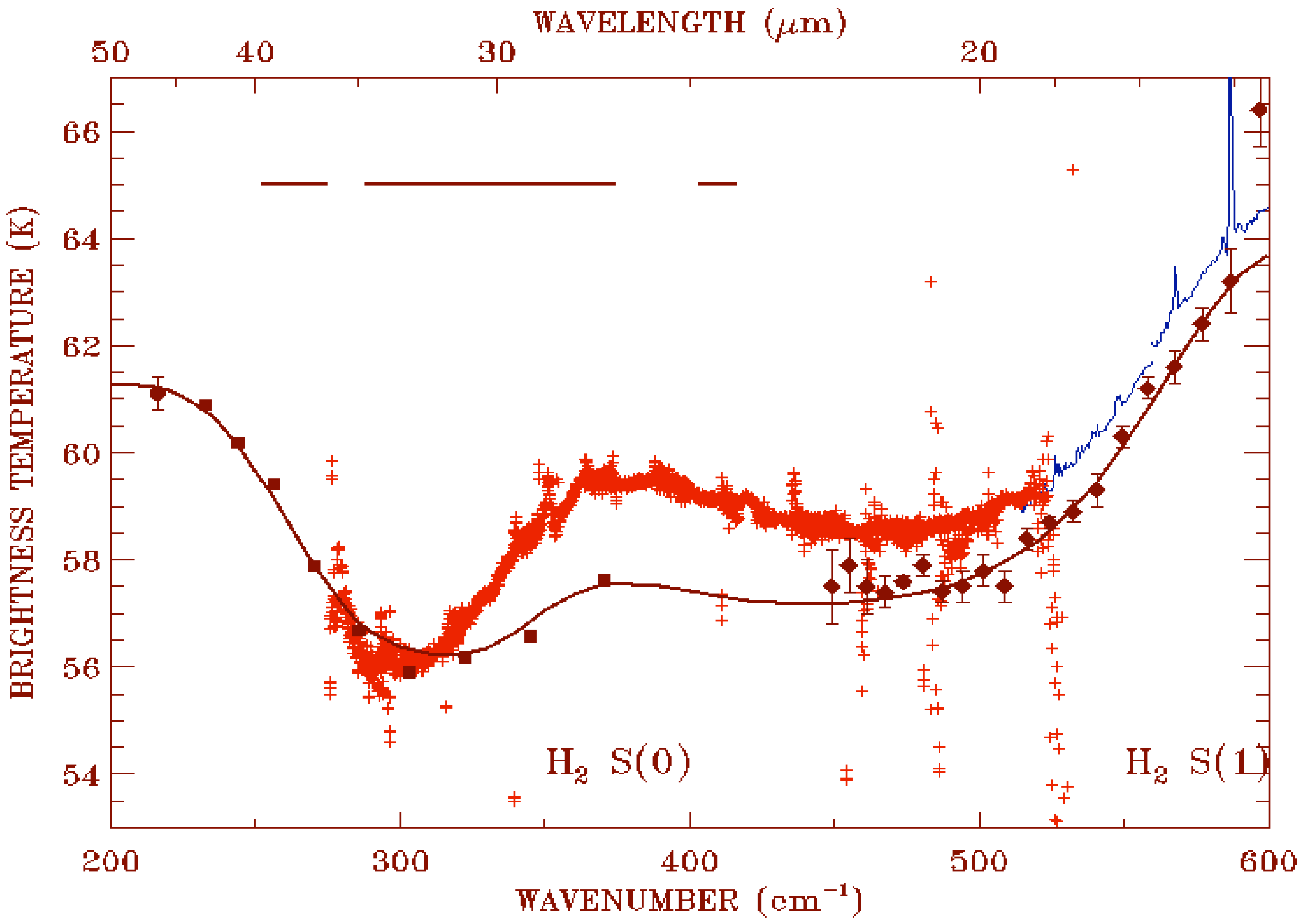

Figure 5-6. *Spectrum of Neptune in the difficult and important mid-IR region unique to SOFIA. The locations of the emission cores of the broad H_2 collision-induced S(0) and S(1) rotational lines are also indicated. Spitzer IRS LH spectral data are red crosses, and SH spectra are the blue lines. A model fitting ground-based data from the 1980s (Orton et al. 1987, diamonds) plus ISO LWS (filled circle) and SWS (filled boxes) data are also shown. Spectral ranges covered by SOFIA FORCAST's 38.0, 30.0, and 24.4 μm broadband filters are shown schematically at the upper left.*